

Essential Characterisation Tools for the Study of MgB₂ Superconductors

Karen A. Yates⁽¹⁾, Yasuyuki Miyoshi⁽¹⁾, James Moore⁽¹⁾, Garry Perkins⁽¹⁾, David Caplin⁽¹⁾, Lesley Cohen and Y. Bugoslavsky⁽²⁾

(1) The Blackett Laboratory, Imperial College, Prince Consort Road, London, SW7 2BZ, England

(2) Cryogenic Limited, The Vale, Acton, London W3 7QE, England

Abstract - We have developed a suite of characterisation tools that have proved invaluable in the ongoing studies of the physical properties of MgB₂ superconductors. Here we highlight the use of combining the measurement of $H_{c2}(T)$ by global magnetometry with measurement of point contact diffusivity, ac calorimetry and Hall probe imaging.

Manuscript received Sept. 26, 2007, accepted October 23, 2007. Reference No. ST9., Category 2

I. INTRODUCTION

Magnesium diboride (MgB₂) is quite an extraordinary superconductor. Simple in physical structure, the complexity of the effective two band (σ and π) superconductivity has generated a great deal of scientific interest. Moreover it seems that many of the materials engineering concepts originally applied to Nb and its alloys can be transferred to the MgB₂ system. It can be made quite easily in a pure form, with low resistivity and long mean free path compared to the coherence length of the larger σ band, and yet simple materials structuring has, at 4.2K, produced impressive results in terms of enhanced upper critical field (H_{c2}) up to ten times larger than in pure single crystals without significant degradation of the critical temperature [1]. Predominantly this improvement in upper critical field results from aspects of the interplay of the double gaps [2] and the intraband scattering that arises from doping and associated lattice distortions.

II. MEASUREMENT OF DIFFUSIVITY IN THIN FILM AND BULK MgB₂ SAMPLES

The multiple band structure of MgB₂ means that three sorts of scattering mechanisms are possible: intraband scattering within the π and σ bands and interband scattering between the two. Interband scattering is associated theoretically [3] and experimentally [4] with a reduction in the T_c of the material and a decrease in the energy separation between the two order parameters Δ_σ and Δ_π . These gap values are directly measurable by point contact Andreev reflection (PCAR) using a mechanically sharpened Au tip as described previously [5]. Measurements of the PCAR as a function of field allow us to fit the spectra, in order to extract a parameter n_π that is a

measure of the number of normal state conducting channels within the point contact [6]. The measurement and “two channel” fitting procedures have been fully described in references [6,7,8]. It has been shown that this parameter n_π can be directly related to the zero bias density of states (DOS) of the π band, N_π , as used in theoretical predictions [6,9].

Gurevich [2] has shown that the $H_{c2}(T)$ dependence is intricately tied to the behaviour of the diffusivity ratio, η . In this work, we define η as D_σ/D_π where D_i are the diffusivities in the σ , π bands. An independent measure of η can be obtained from the n_π as determined from the field-dependent PCAR spectra. To our knowledge, a direct comparison has not been undertaken on the same samples of the values of η obtained by fitting $H_{c2}(T)$ data to the model of reference [2] and the two channel fitting of the PCAR data. In order to test this, we compare results of the η determination from PCAR on a well orientated thin film and that obtained by fitting the $H_{c2}(T)$ at $T \sim T_c$ of the same film. The PCAR technique was then applied to the measurement of bulk polycrystalline samples, one of which was nominally pure and the other with a small percentage of Al doping.

By fitting the PCAR data of a c-axis orientated MgB₂ thin film, as described in [6], a value of $\eta = 0.5$ was obtained. The $H_{c2}(T)$ was determined resistively for the same film in reference [5]. To determine η from the $H_{c2}(T)$ based on the model of Gurevich [2], we have used the formula for the gradient of $H_{c2}(T)$ at $T \sim T_c$ as described by Putti et al [10]:

$$\left. \frac{dH_{c2,ab}}{dT} \right|_{T_c} = \frac{16\phi_0 k_B}{\pi \hbar \mu_0} \frac{1}{(a_1 D_\sigma / \gamma) + a_2 D_\pi}$$

here ϕ_0 is the magnetic flux quantum, γ is taken to be the H_{c2} anisotropy and a_1 and a_2 are proportional to the coupling constants, λ_{ij} . For pure MgB₂, $a_{1,2}$ have been calculated [2,3,10] to be $a_1 = 1.93$ and $a_2 = 0.07$. Following the method set out in reference [10] we find that $\eta = 0.1 \pm 0.06$ if we set $\gamma = 4$. While this value is smaller than that found by PCAR, we note that the values are consistent to within an order of magnitude. Considering that η varies over several orders of magnitude [2,9,11,12] we believe that this supports the validity of the point contact methodology. Further comparison of the two methods would be possible were the entire $H_{c2}(T)$ curve obtained and fitted.

Having discussed the agreement of the value for η determined by both methods, we turn our attention to the bulk polycrystalline samples. First we show the distribution of gap values in two bulk polycrystalline samples one which is nominally pure and the other with a small percentage of Al doping. The Al doped and pure samples were prepared as described elsewhere [13]. It has been shown [14] that Al doping fills the σ bands leading to a rapid decrease in T_c with Al doping. It has also been shown [13] that even small amounts of Al doping can lead to structural modifications such as the introduction of Mg vacancies. It is therefore clear that Al doping and preparation technique can have a considerable influence on MgB₂, with both band filling and disorder-induced scattering playing a role in the superconducting properties T_c , J_c , H_{c2} of the material.

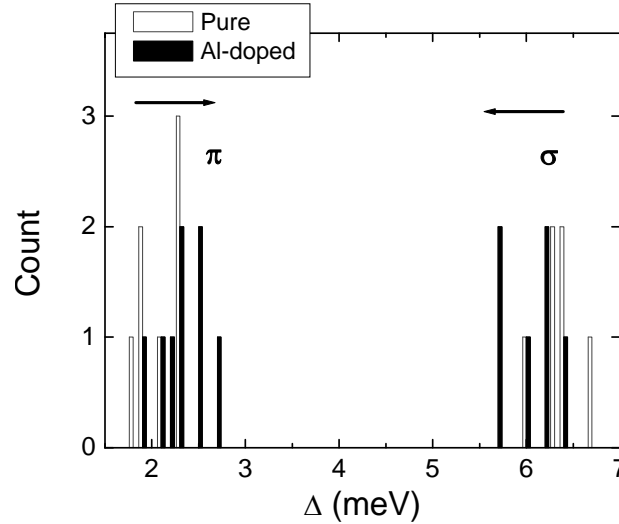


Fig. 1. Statistical analysis of the Andreev reflection spectra showing the position of the value of the energy gaps from many different sampling positions in a) pure MgB₂ and b) 1% Al doped MgB₂ at T=4.2 K.

The behaviour of the gaps measured by point contact Andreev spectroscopy will be different depending on the type of dopant added to the MgB₂ [4]. If band filling occurs, such as would be the case with the hole dopant Al³⁺, both gaps would decrease in energy with doping. Conversely, significant interband scattering as a result of the dopant, would lead to the two gaps converging as the T_c is reduced [4]. In general, either or both effects can influence the variation of the gaps with the dopant concentration and different effects have been reported for the same dopant [4]. The values of $\Delta_{\pi,\sigma}$ extracted from a number of spectra at different locations on the bulk surface of both samples are shown in the histogram in Figure 1. The spread of the gap values measured by point contact spectroscopy may in part be due to sample inhomogeneity. Though as can be seen from the statistics in figure 1, the distributions of the two gaps measured in the Al doped sample are moderately closer together than in the undoped sample suggesting a moderate increased interband scattering, consistent with the decreased T_c observed in this 1% Al doped sample.

In order to estimate the diffusivity ratio of the two bands, point-contact spectra in applied magnetic field were taken. The spectra, as a function of field, were fitted to the two channel model as previously described in references [6,7,8,15]. Although the model of Koshelev and Golubov [9] is only strictly valid for fields applied parallel to the c-axis, we and others have shown that the model can be applied to bulk samples as the π band is relatively isotropic at low fields [6,8,15]. In Figure 2a we show the density of states for both bands compared to the theory for a value of $\eta = 0.3$. In order to do this, an H_{c2} value of ~ 16 T was used, based on bulk magnetometry data. Given the uncertainty in H_{c2} , the obtained σ band DOS has a large uncertainty. On the contrary, the fit result for the π band DOS is much less dependent on the orientation of the external field with respect to the crystal planes. Nevertheless fitting the $H_{c2}(T)$ at $T \sim T_c$ of the undoped sample with the model of Gurevich [2,10] gives very similar values of η to that obtained by PCAR. In this case, because the residual resistivity is unknown, we have used the values of $D_{\sigma,\pi} \sim 1.7 \times 10^{-3} \text{ms}^{-1}$ found by Putti et al [10]. By varying the anisotropy between 2 and 4, typical for MgB₂ and altering $D_{\pi,\sigma}$ slightly to fit the gradient of H_{c2} at $T \sim T_c$, we find that $0.26 \leq \eta \leq 0.52$.

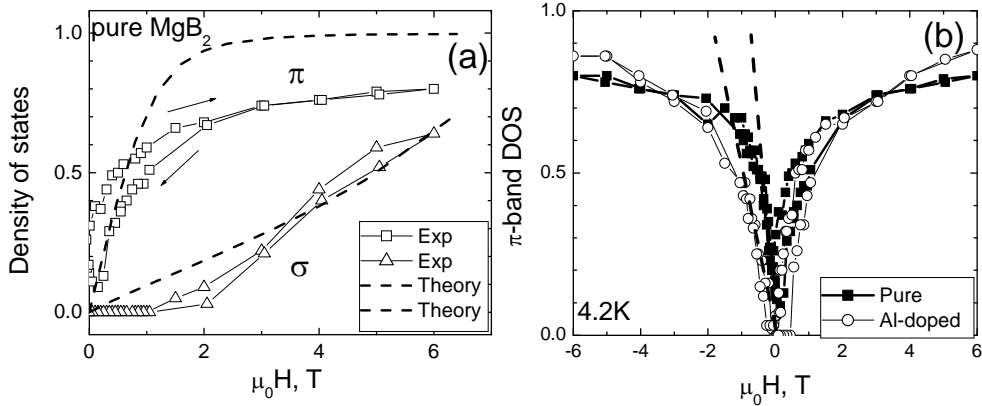


Fig. 2. a) The experimentally extracted and theoretically predicted values of the DOS. The sample used in this case was pure MgB_2 . The theory assumes that the field is applied along the c -axis; the sample is however randomly oriented and the contact probes all possible directions. We show the behaviour of both the σ and the π band DOS averaged over all field orientations. b) The DOS for the π band only for both the un-doped and doped sample.

The π band DOS for the undoped and 1% Al doped sample is shown in Figure 2b on a non-reduced magnetic field scale because the two samples had the same global $H_{c2}(T)$ values. We anticipate that when the relative scattering of the π band increases, that is, for higher values of η , the gradient of the N_π DOS becomes shallower with field [9]. There is indeed a difference in the slope at low field between the Al-doped and the undoped samples; it may indicate that Al-doping has increased the diffusivity ratio, that is, made the π band ‘dirtier’ with respect to the σ .

III. CALORIMETRY AND MAGNETOMETRY OF SINGLE CRYSTALS AND BULK MgB_2

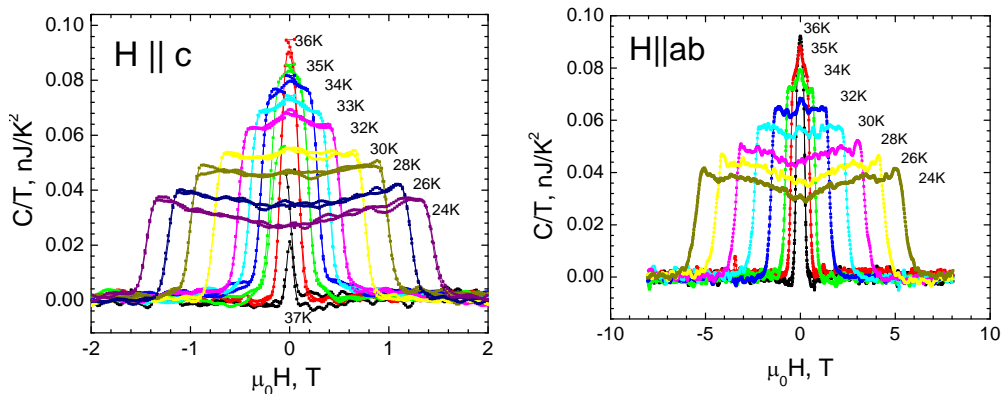


Fig. 3. Heat capacity of the pure MgB_2 crystal as a function of the magnetic field applied parallel to the c axis (left) and along the ab plane (right). The data is taken at different temperatures as indicated on the graph.

MgB_2 is anisotropic, so that calorimetric studies should be made on single crystals. However, only rather small (sub-millimetre) MgB_2 crystals can be grown. Because of the technical difficulties, there have been only a few calorimetric studies of such small

crystals [16,17]. We have recently developed an ac-nanocalorimetry technique suitable for this purpose [18]. Its key element is a miniature commercial sensor (Xensor Integration [19]), in which a resistive heater and a sensitive thermopile are integrated on a silicon nitride membrane. The technique has a noise level approaching pJ/K, and so can be used with samples in the microgram range; furthermore, measurements can be made in high magnetic fields.

Calorimetry provides the most reliable measurement of H_{c2} and for the purposes of this paper this is the information we extract from the data in Figure 3. Here we are only interested in the magnetic field at which there is a step change in the heat capacity. If the H_{c2} step transition is not sharp we can define two fields: the onset to the H_{c2} transition, which we denote as H_1 , and the completion of the transition, H_2 . It is surprising that even in single crystals we see a significant slope to the H_{c2} transition. The definition of H_1 and H_2 is shown in the inset to Figure 4.

There is a great deal of additional information that can be extracted from such data, particularly if the size of the heat capacity jump is properly calibrated. We mention this for completeness only, because such analysis is beyond the scope of the current work. Examples of extremely rich physics that can be accessed from heat capacity include: extracting information on the different pair breaking rates associated with the two gaps [20]; the deviation from pure anisotropic Ginzburg-Landau predictions of the angular dependence of H_{c2} [21]; and observation of the crossover to single-gap superconductivity upon carbon doping [22].

The evolution of the heat capacity jump with field shown in Figure 3 results from MgB_2 being a high- κ type II superconductor. The heat capacity jumps in the Messiner state ΔC_0 and in the mixed state ΔC are related by [23]

$$\lim_{T \rightarrow T_c} \frac{\Delta C}{\Delta C_0} = \frac{2\kappa^2}{\beta(2\kappa^2 - 1)}$$

where the Abrikosov parameter β is 1.159 for a triangular lattice. In the limit $\kappa \gg 1$, the heat capacity ratio above is ~ 0.86 , whereas the measured ratio for $H \parallel ab$ in Fig. 3 yields ~ 0.92 at 36K, close to the T_c of 38K. Furthermore, we observe a small peak near H_{c2} which is linked to the peak effect (softening of the vortex lattice near H_{c2}). The effect is more pronounced in $H \parallel ab$ than in $H \parallel c$ geometry due to anisotropic vortex dynamics in MgB_2 .

The anisotropy of H_{c2} has important implications for the behaviour of MgB_2 tapes and wires, which are of necessity polycrystalline. J_C becomes zero at a somewhat smaller field H_{irr} , which is signalled in magnetometry by the loss of irreversibility. Interestingly, we find a close correlation between the magnetic and calorimetric responses of *bulk* material (see Figure 4): the heat capacity begins its transition at a field that is close to the magnetometric H_{irr} , that is, when the applied field reaches the H_{c2} of the grains that are oriented close to the least favourable direction ($H \parallel c$); thus large-scale currents can no longer percolate through the sample. The completion of the heat capacity transition and the disappearance of the last vestiges of a diamagnetic signal correspond of course to grains for which $H \parallel ab$.

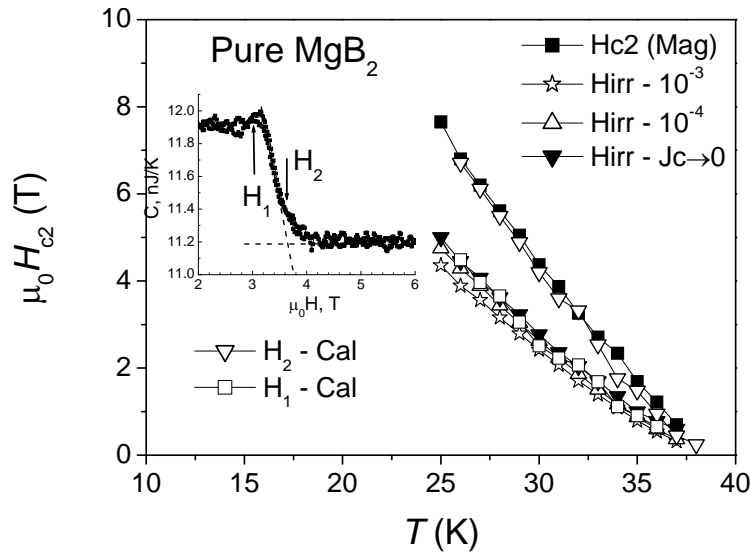


Fig. 4. Upper critical field H_{c2} vs temperature, T , extracted from complementary magnetometry and calorimetry measurements on a bulk polycrystalline sample. The inset shows how the upper critical field is extracted from the step like change that we observe in calorimetry. See text for details explaining H_1 and H_2 . Also shown is the H_{irr} vs T extracted from the magnetisation loop using various threshold values of the critical current as indicated on the figure legend. The H_{irr} line is not very sensitive to the threshold value but lies close to the onset of the upper critical field.

IV. CONNECTIVITY OF BULK MgB_2 AND MgB_2 SHEATHED TAPES, USING ac SUSCEPTIBILITY AND HALL PROBE IMAGING

It is well-known that the current-carrying capacity of bulk polycrystalline MgB_2 is degraded by porosity, and also by imperfect grain contact; furthermore, both of these factors may vary across the sample. In assessing MgB_2 conductors it is important to gauge the magnitude of these macroscopic factors, so as to be able quantify the intrinsic critical current density and flux pinning.

A quick check on the sample connectivity can be made using the long-established length-scale technique [24]. For MgB_2 materials, we have modified it slightly (by incorporating a small ac magnetic field in our 8 T VSM, and so measuring the ac magnetic susceptibility as a function of the dc applied field), so as to increase its sensitivity in high fields.

We obtain much more detailed maps of spatial homogeneity with our scanning Hall probe microscope, [25] in magnetic fields up to 4 T (in contrast, magneto-optic imaging is limited to much lower fields, because the indicator films saturate). Its spatial resolution is a few microns, and the images can be correlated directly with optical and SEM micrographs. Figure 5 shows images on a 5% carbon-doped MgB_2 bulk superconductor. Other results on these samples are given in [26].

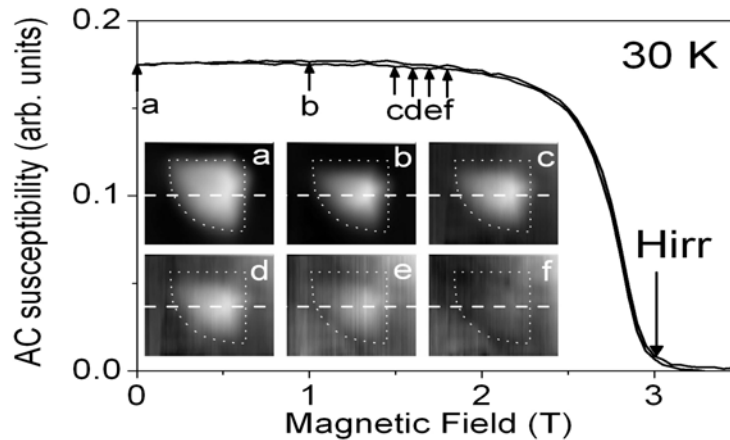


Fig. 5. An example of ac magnetic susceptibility vs applied field curve at 30 K for bulk MgB_2 . The irreversibility field H_{irr} is defined by extrapolating to zero the sharp decrease in susceptibility observed at high field. This type of measurement also indicates the length-scale over which the current is flowing in the sample [24]. Inset shows $4\text{mm}\times 4\text{mm}$ scanning Hall probe images of sample M06 at 30 K (dotted line indicates the sample border) at the constant applied fields labelled (a) to (f). The greyscale contrast shows variation of magnetic induction across the image window (black corresponds to regions of approximately zero induction and white to regions of high induction). See [26] for more details.

V. SUMMARY

We have given an overview of a suite of characterisation tools which can be used to examine fundamental aspects of superconducting materials and extrapolate the behaviour of key parameters and how they impact on the technologically relevant parameters H_{irr} , H_{c2} and J_c .

ACKNOWLEDGEMENTS

We thank the providers of samples. Andrew Berenov and Judith Driscoll who made the bulk samples, and S. Lee who provided the single crystal samples discussed here.

REFERENCES

- [1] V. Ferrando, P. Orgiani, A. V. Pogrebnikov *et al*, *Appl. Phys. Lett.* **87**, 252509 (2005)
- [2] A. Gurevich – cond Mat 070128 Jan 12th 2007; A. Gurevich *Phys Rev B* **67** (2003) 184515
- [3] A. Liu, I. Mazin, J. Kortus, *Phys. Rev. Lett.* **87**, 087005 (2001)
- [4] J. Kortus, O. Dolgov, A. Golubov, *Phys. Rev. Lett.*, **94**, 027002 (2005)
- [5] Y. Bugoslavsky, Y. Miyoshi, G.K. Perkins, A.D. Caplin, L.F. Cohen, A.V. Pogrebnikov, X.X. Xi, *Phys. Rev. B*, **69**, 132508 (2004)
- [6] Y. Bugoslavsky, Y. Miyoshi, G.K. Perkins, A.D. Caplin, L.F. Cohen, *Phys. Rev. B*, **72**, 224506 (2005)
- [7] Y. Miyoshi, Y. Bugoslavsky, L.F. Cohen, *Phys. Rev. B*, **72**, 012502 (2005)
- [8] K.A. Yates, Y. Miyoshi, J. Grunwell, K. Riggall, L.F. Cohen, S.K. Chen, J.L. MacManus Driscoll, A. Serquis, *Appl. Phys. Lett.* **91**, 122501 (2007)
- [9] A. Koshelev, A. Golubov, *Phys. Rev. Lett.*, **90**, 177002 (2003)

-
- [10] M.Putti, V.Braccini, C. Ferdeghini, I. Pallecchi, A. S. Siri, F. Gatti, P. Manfrinetti, A. Palenzona, *Phys. Rev. B* **70**, 052509 (2004)
 - [11] A.Gurevich, S.Patnaik, V.Braccini, *et al*, *Supercond. Sci. Technol.*, **17**, 278 (2004)
 - [12] M.-S. Park, H.-J.Kim, B. Kang, S.I. Lee, *Supercond. Sci. Technol.* **18**, 183 (2005)
 - [13] A. Berenov, A. Serquis, X.Z. Liao *et al*, *Supercond. Sci. Technol.* **17** 1093, (2004)
 - [14] J.M. An and W.E. Pickett, , *Phys. Rev. Lett.*, **86**, 4366 (2001)
 - [15] P.Szabo, P.Samuely, Z.Pribulova, M.Angst, S.Bud'ko, P.C. Canfield, J. Marcus, *Phys. Rev. B*, **75**, 144507 (2007)
 - [16] T. Klein, L. Lyard, J. Marcus, *et al*, *Phys. Rev. B* **73**, 224528 (2006).
 - [17] Z. Pribulova, T. Klein, J. Marcus, *et al*, *Phys. Rev. Lett.* **98**, 137001 (2007).
 - [18] A.A.Minakov, S.B.Roy, Y.V.Bugoslavsky, L.F.Cohen, *Rev Sci Instr* **76**, 043906 (2005)
 - [19] www.xensor.nl
 - [20] F.Bouquet, Y.Wang, I.Sheikin, T.Plackowski, A.Junod, S.Lee, S.Tajima. *Phys Rev Lett* **89**, 257001 (2002)
 - [21] A. Rydh, U. Welp, A. E. Koshelev,*et al*, *Phys. Rev. B* **70**, 132503 (2004)
 - [22] M.Putti, M.Affronte, C.Ferdeghini, M.Manfrinetti, C.Tarantini, E.Lehmann, *Phys Rev Lett* **96**, 077003 (2006)
 - [23] R. Radebaugh and P. H. Keesom, *Phys. Rev.* **149**, 217 (1966).
 - [24] MA Angadi *et al*, *Physica C* **177** (1991) 476; A. D. Caplin, M. A. Angadi, J. R. Lavery, and A. L. Deoliveira, *Superconductor Science & Technology* **5**, S161-S164 (1992).
 - [25] G. K. Perkins *et al.*, *IEEE Transactions on Applied Superconductivity* **11**, 3186 (2001).
 - [26] J.D. Moore, G.K. Perkins, W. Branford *et al*, *Supercond. Sci. Technol.* **20**, S278 (2007)